11

A Facial Expression Imitation System for the Primitive of Intuitive Human-Robot Interaction

Do Hyoung Kim[†], Kwang Ho An[2], Yeon Geol Ryu[2] and Myung Jin Chung[2]
[1]*Mobile Communication Division, Samsung Electronics Co.*
[2]*Electrical Engineering Division, Korea Advanced Institute of Science and Technology*
Republic of Korea

1. Introduction

The human face has long been considered a representation of humans. According to observations of cognitive psychology, people unconsciously and frequently recognize and identify others from their faces. Many researchers have also emphasized the importance of the human face, e.g., Cicero said "Everything is in a face," Darwin stated that "The human face is the most complex and versatile of all species," and Paul Ekman remarked "The face makes one's behavior more predictable and understandable to others and improves communication" (Kim et al., 2005).

Nobody doubts that the human face is a rich and versatile instrument that serves many different functions and conveys the human's motivational state. Facial gestures can communicate information on their own. Moreover, the face serves several biological functions; for instance, humans generally close their eyes to protect themselves from a threatening stimulus, and they close them for longer periods to sleep (Breazeal, 2004) (Mcneill, 1998) (Ekman et al., 2002).

To interact socially with humans, a robot must be able to do gather information about its surroundings as well as express its state or emotion, so that humans will believe that the robot has beliefs, desires, and intentions of its own. Cynthia Breazeal who is one of pioneers on the natural and intuitive HRI research at MIT mentioned the ideal robotic system like this: "The ideal of the robotic system is for people to interact, play and teach the robot as naturally as they would teach an infant or a very young child. Such interactions provide many different kinds of scaffolding that the robot can potentially use to foster its own learning. As a prerequisite for human-robot interactions, people need to ascribe precocious social intelligence to the robot. However, before people treat the robot as a socially aware being, the robotic system need to convey subjective internal states such as intentions, beliefs, desires, and feelings" (Breazeal, 2004). As a result, facial expressions are critical in a robotic system because they encourage people to treat the robot as an object that can convey internal states, have social intelligence and exploit human-like tendencies.

Our facial expression imitation system is composed of two modules, which are facial expression recognition and facial expression generation (see Figure 1). The system firstly detects human's face in the image. The proposed facial expression recognition algorithm classifies the obtained face into one of P. Ekman's basic facial expressions that include

Source: Human-Robot Interaction, Book edited by Nilanjan Sarkar,
ISBN 978-3-902613-13-4, pp.522, September 2007, Itech Education and Publishing, Vienna, Austria

neutral, happiness, sadness, anger, surprise, disgust and fear (Ekman et al., 2002). From the result of the recognition, our facial expression imitation system knows user's facial expression, and it copies the recognized facial expression through the following procedures: artificial facial expression generation, multiple motor control, and movements of robot's eyelid and mouth.

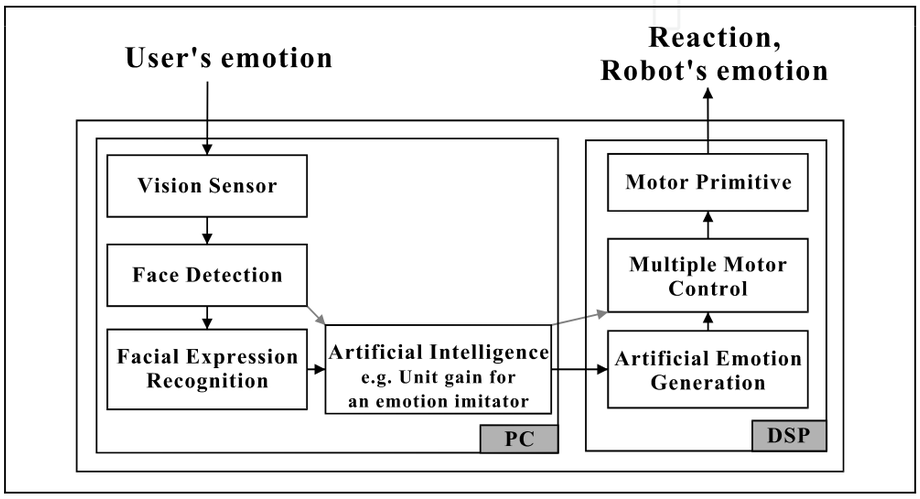

Figure 1. The whole system block diagram. The image pre-processing, face detecion and facial expression recognition algorithm run on a personal computer (PC) with a commercial microprocessor. In addition, the generation of robot's facial expression and motor controller operate in a fixed point digital signal processor (DSP)

For the facial expression recognition, we introduced new types of rectangle features that can distinguish facial expressions efficiently with consideration of more complicated relative distribution of facial image intensities. In order to find the rectangle features that have the highest recognition rate, we firstly selected the efficient rectangle feature types for facial expression recognition from all possible rectangle feature types in a 3×3 matrix form using 1065 facial expression images based on the JAFFE (Japanese Female Facial Expression) database. Each rectangle feature type was selected by the AdaBoost algorithm. We then measured the error rate and chose the top five rectangle feature types that had the least error rate among the total 316 rectangle feature types for each facial expression.

For the facial expression generation, we have designed our system architectures to meet the challenges of real-time visual-signal processing and real-time position control of all actuators with minimal latencies. The motivational and behavioral parts run on a fixed point DSP and 12 internal position controllers of commercial RC servos. 12 actuators are able to simultaneously move to the target positions by introducing a bell-shaped velocity control. The cameras in the eyes are connected to the PC by the IEEE 1394a interface, and all position commands of actuators are sent from PC.

2. Contents of the Chapter

This Chapter has attempted to deal with the issues on establishing a facial expression imitation system for natural and intuitive interactions with humans. Several real-time cognition abilities were implemented such as face detection, face tracking, and facial expression recognition. Moreover, a robotic system with facial components is developed, which is able to imitate human's facial expressions.

As briefly mentioned above, two major issues will be dealt with in this Chapter; one is the facial expression recognition and the other is the facial expression generation. In the recognition part, the following contents will be included.

- The state-of-the-art for automatically recognizing facial expressions of human being.
- Issues for the facial expression recognition in the real-time sense.
- The proposed recognition approach.

In order to recognize human's facial expressions, we suggested a method of recognizing facial expressions through the use of an innovative rectangle feature. Using the AdaBoost algorithm, an expanded version of the process with the Viola and Jones' rectangle feature types has been suggested. We dealt with 7 facial expressions: neutral, happiness, anger, sadness, surprise, disgust, and fear. Real-time performance can be achieved by using the previously trained strong classifier composed by a set of efficient weak classifiers.

In the generation part, the following contents will be included.

- The state-of-the-art for facial robots.
- Issues for designing and developing facial robots; e.g. the mechanics, the system architecture, and the control scheme.
- Issues for image processing and visual tracking.
- Introduction of the developed facial robot and the generation method of facial expressions.

In addition, several experiments show the validity of the developed system. Finally, some conclusions and further works are presented.

3. Facial Expression Recognition

To date, many approaches have been proposed in the facial expression recognition field. According to which factor is considered more important, there are many categorizations (Pantic & Rothkrantz, 2000) (Fasel & Luettin, 2003). Based on facial expression feature extraction, we can classify previous approaches as model-based methods or image-based methods.

As a representative model-based method, Essa and Pentland fitted a 3D mesh model of face geometry to a 2D face image and classified five facial expressions using the peak value of facial muscle movement (Essa & Pentland, 1997). Lanitis et al. used Active Appearance Models (AAM) to interpret the face and Huang and Huang used a gradient-based method to classify face shape using a Point Distribution Model (PDM) (Lanitis et al., 1997) (Huang & Huang, 1997). Zhang et al. fitted the face with sparsely distributed fiducial feature points and distinguished facial expressions (Zhang et al., 1998). Generally, these model-based methods are robust to occlusions. However they are inadequate for a real-time system because they require much time to fit the model to the face image and need high resolution input images to analyze facial expressions.

Among the image-based methods, Lisetti and Rumelhart used the whole face as a feature and Fellenz et al. used Gabor wavelet filtered whole faces (Lisetti & Rumelhart, 1998) (Fellenz et al., 1999). Padgett and Cottrell extracted facial expressions from windows placed around the eyes and mouth and analyzed them using Principle Components Analysis (PCA) (Padgett & Cottrell, 1997). Bartlett distinguished facial expressions using an image intensity profile of the face and Lien et al. used dense flow with PCA and block based density to classify facial expressions (Bartlett, 1998) (Lien et al., 1998).

Recently, Viola and Jones constructed a fast face detection system using rectangle features trained by the AdaBoost algorithm (Viola & Jones, 2001) (Freund & Schapire, 1995). Wang et al. applied this method to facial expression recognition and distinguished 7 class facial expressions in real-time (Wang et al., 2004). However, the systems implemented by AdaBoost used Haar-like rectangle features for face detection or a bit modified rectangle features (Wang et al., 2004) (Littlewort et al., 2004). More analysis and innovative rectangle features should be established for facial expression recognition. Because the rectangle features consider a local region of the face, new rectangle feature types are needed to consider more complicated relative distribution of facial image intensities for facial expression recognition.

Given 7 facial expressions (neutral, happiness, anger, sadness, surprise, disgust, fear), we obtained discernable rectangle feature types for each facial expression among all possible rectangle feature types in 3×3 matrix form. The rectangle features are selected again from the facial image database using the AdaBoost algorithm with the above rectangle feature types, and so improved the recognition rate of a strong classifier and automatically and spontaneously recognized human facial expressions in real-time.

3.1 Viola and Jones' Boosting Method; AdaBoost Algorithm

AdaBoost learning algorithm is a simple learning algorithm that selects a set of efficient weak classifiers from a large number of potential features. Our boosting algorithm is basically the same as Viola and Jones' boosting algorithm (Viola & Jones, 2001). From this procedure, T weak classifiers are constructed and the final strong classifier is a weighted linear combination of the T weak classifiers.

- Consider sample images $(x_1, y_1), \ldots, (x_n, y_n)$, where $y_i = 0, 1$ for negative and positive samples, respectively.
- Initialize weights $w_{1,i} = \frac{1}{2m}, \frac{1}{2l}$ for $y_i = 0, 1$, respectively, where m and l are the number of negatives and positives, respectively.
- For $t = 1, \ldots, T$,
  1) Normalize the weights so that w_t is a probability distribution.

$$w_{t,i} \leftarrow \frac{w_{t,i}}{\sum_{j=1}^{n} w_{t,j}} \tag{1}$$

  2) For each feature, j, train a weak classifier h_j.

$$\varepsilon_j = \sum_i w_i \left| h_j(x_i) - y_i \right| \cdot \tag{2}$$

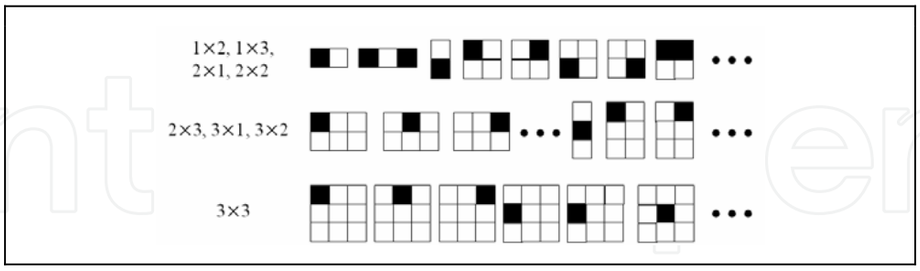

Figure 2. All possible rectangle feature types within up to 3×3 structure size used for training

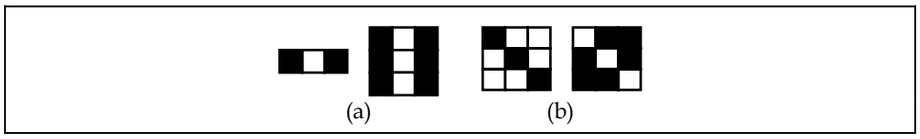

Fig. 3. Examples of overlapped rectangle feature types. (a) The types are independent of size variation, (b) The types consider unsigned feature value.

3) Choose the classifier h_t with the lowest error ε_t.

4) Update the weights.

$w_{t+1,i} = w_{t,i}\beta_t^{1-e_i}$, where $e_i = 0$ if sample x_i is classified correctly, $e_i = 1$ otherwise.

- The final strong classifier is

$$H(x) = \begin{cases} 1 & , if \sum_{t=1}^{T} \alpha_t h_t(x) \geq 0.5 \times \sum_{t=1}^{T} \alpha_t \\ 0 & , \quad otherwise \end{cases}, \quad \alpha_t = \log \frac{1}{\beta_t}. \tag{3}$$

3.2 Procedure for Feature Type Extraction

The process of extracting weak classifiers is identical to Viola and Jones method. Using the selected rectangle feature types, we trained a face training image set and constructed a strong classifier for each facial expression. Before the procedure of extracting classifiers, suitable feature types for facial expression recognition are extracted from all possible rectangle feature types within a 3×3 matrix form as follows.

- Find all possible rectangle feature types within a 3×3 matrix form. (See Figure 2.)
- Among the above rectangle feature types, exclude overlapped feature types.

1. Size variation

Though two rectangle feature types in Fig. 3(a) have different shapes, they are overlapped when searching a weak classifier because the size of the rectangle feature can be extended in the x, y directions.

2. Feature value

Fig. 3(b) shows rectangle feature types that have the same feature values and opposite polarity. Since the AdaBoost algorithm is a two-class classification method, the two rectangle feature types in Fig. 3(b) have the same function.

- For p = 1, …, # *of facial expression classes*,
  Consider sample images (x_1, y_1), …, (x_n, y_n) where y_i = 1, 0 for the target facial expression images and the other facial expression images, respectively. Q denotes the total number of rectangle feature types.
- For q = 1, …,*Q*,
  Initialize weights $w_i = \frac{1}{2m}, \frac{1}{2l}$ for y_i = 1, 0, respectively, where m and l are the number of the target facial expression images and the other facial expression images.
  - For t = 1, …,T,
    1. Normalize the weights so that w_t is a probability distribution.

$$w_{t,i} \leftarrow \frac{w_{t,i}}{\sum_{j=1}^{n} w_{t,j}}$$

    2. For each the feature, j, based on q^{th} rectangle feature types, train a weak classifier h_j.

$$\varepsilon_j = \sum_i w_i \left| h_j(x_i) - y_i \right| .$$

    3. Choose the classifier $h_{q,t}$ with the lowest error $\varepsilon_{q,t}$.
    4. Update the weights.
       $w_{t+1,i} = w_{t,i}\beta_t^{1-e_i}$, where e_i = 0 if sample x_i is classified correctly, e_i = 1 otherwise.
    5. Calculate $\alpha_{p,q,t}$ as followings:

$$\alpha_{p,q,t} = \log \frac{\varepsilon_{q,t}}{1-\varepsilon_{q,t}} . \tag{4}$$

- Sort $\alpha_{p,q,t}$ in high value order for each p and choose rectangle feature types that have high $\alpha_{p,q,t}$ value.

3.3 Selected Rectangle Features

Fig. 4 shows the rectangular feature types that effectively distinguish the corresponding facial expressions extracted from the results of boosting algorithm. In this figure, we arrange the features in order of the least error from left to right. In Fig. 4, the facial image is place in a position such that the facial expression can be most accurately distinguished. And the best rectangular feature is overlay to the corresponding facial expression image. As you can see in Fig. 4, almost all of the features consider the area just above the mouth, cheek and the white of the eye. This is because we considered the phenomenon that when a person smiles or becomes frustrated or annoyed, he or she tends to alter the expression of the mouth or area around the eyes.

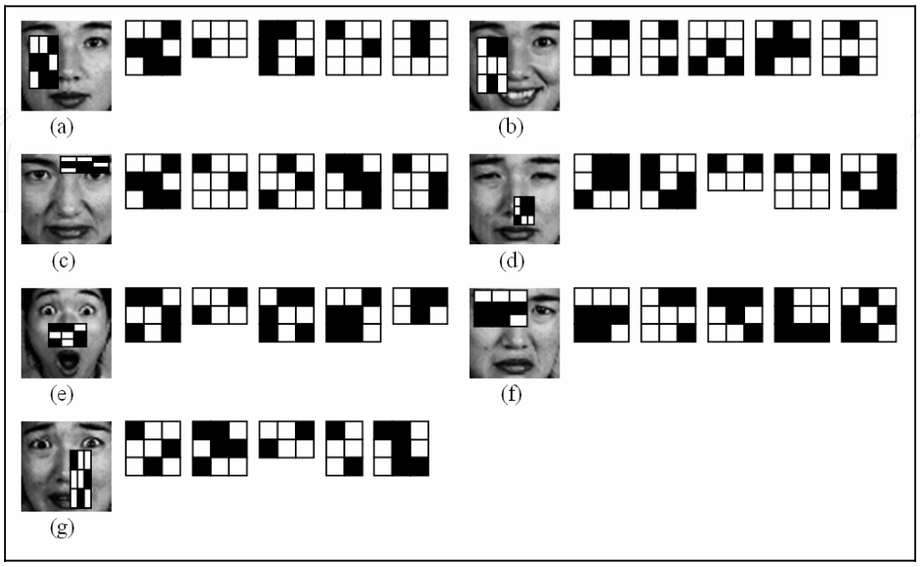

Figure 4. 5 selected rectangle feature types for each facial expression . (a) neutral, (b) happiness, (c) anger, (d) sadness, (e) surprise, (f) disgust, (g) fear

In Fig. 4(a), 5 feature types that distinguish the 'neutral' facial expression from other facial expressions are shown. As you can see in this figure, they consider the area above mouth, cheek and the white of the eye. Fig. 4(b) shows five types that characterize the 'happy' facial expression and the rectangular feature with the least error rate. In Fig. 4(b), the features consider the eye and mouth of the smiling facial expressions. Fig. 4(c) shows the rectangular feature that most effectively distinguishes the expression of 'anger'. The angry facial expression is characterized by a change in the shape of the eyebrows. It has V shape eyebrows and the area between eyebrows appears wrinkled. In Fig. 4(c), the rectangle feature that distinguishes the angry face considers both the eyebrows and the area between eyebrows. Fig. 4(d) shows the rectangular feature that most effectively distinguishes the expression of 'sorrow'. According to Ekman's research, the edge of the lip moves downwards and the inner part of the eyebrows pull toward each other and move upward (Ekman et al., 2002). Meanwhile, the skin area under the eyebrows becomes triangular in shape. However, Fig. 4(d) does not consider these features, because the features that characterize the facial expression of sorrow are very weak and are not adequate to distinguish this expression. Therefore, in Fig. 4(d), we present the rectangular feature obtained by learning that has highest detection rate. Fig. 4(e) presents the best feature that effectively distinguishes the 'surprise' facial expression. There are a number of features that characterize the expression of surprise. In Fig. 4(e) the good features are placed around the nose. In general, when surprised he or she opens his or her eyes and mouth. This pulls the skin under the eyes and around the mouth, making these areas become brighter. Fig. 4(e) shows the selected feature considers this kind of area precisely. The expression of disgust is difficult to distinguish, because it varies from person to person and the degree of the expression is different from one person to another. In particular, it is hard to distinguish this

expression from the expression of anger. In Fig. 4(f), among the rectangular features obtained by boosting algorithm, the one that most effectively distinguishes the expression of 'disgust' is presented. This rectangular feature considers the wrinkles around the eyes and nose. Fig. 4(g) presents the rectangular feature to distinguish the 'fear' facial expression. The expression of fear is the hardest to distinguish. Therefore, we have obtained the fear rectangle feature types through learning. Five rectangular features are shown in Fig. 4(g).
Previously listed rectangle features represent the characters of the facial expressions of Ekman's research (Ekman et al., 2002). Above rectangle feature types consider not only more than two face features but also the character of each emotion.

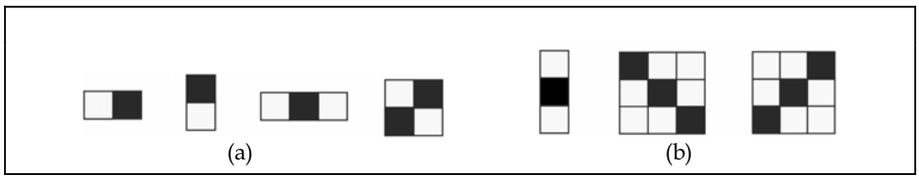

Figure 5. Modified rectangular features. In (a), four types of rectangular features which are proposed by Viola and Jones are shown. Two additional types to focus on diagonal structures and a type for the vertical structure in the face image are shown in (b)

3.4 Selected Feature Analysis

The previous section shows that 35 types of rectangle features are reasonable for classifying facial expressions. This section verifies that the selected rectangle feature types yield better performance than 7 types of rectangle features (four of Viola and Jones (Viola & Jones, 2001) and three of diagonal rectangle feature types in Fig. 5). At first using 7 rectangle feature types, we found the discernable rectangle feature types by using facial expression images in the same manner as that outlined in Section 3.2. Secondly, through application of the best discernable rectangle features to the same images and comparison of the feature values, we conduct a qualitative analysis.

Weak Classifier Comparison

To compare the recognition rate of the weak classifiers, Fig. 6(a) shows a rectangle feature that effectively distinguishes the neutral facial expression among the 7 rectangle feature types and Fig. 6(b) presents the best discernable feature type among the 35 rectangle feature types. These are applied to all facial expression images. Each feature value (the intensity difference between the intensity of the white rectangle and the intensity of the block rectangle) for each facial expression is indicated in Fig. 7. Fig. 7(a) shows the feature values in case of Fig. 6(a) and Fig. 7(b) shows the results of Fig. 6(b). The dotted line in Fig. 7 is the threshold value obtained by using AdaBoost algorithm. As seen in Fig. 7, the method using 7 rectangle feature types doesn't distinguish exactly between neutral facial expression and non-neutral expressions. But the method using 35 rectangle feature types can distinguish between neutral expression and other expressions even if using a weak classifier. However, because this analysis is only for one weak classifier, it can not be sure that the recognition rate of the strong classifier is improved. Nevertheless, if each recognition rate of the weak classifier is improved, we can say that the recognition rate of the strong classifier will be improved.

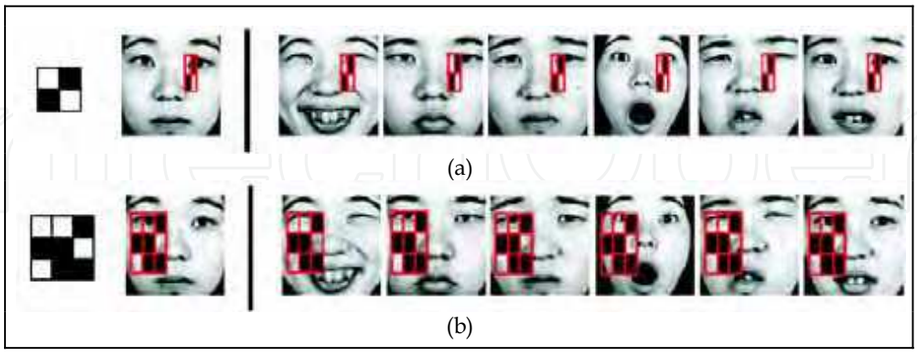

Figure 6. Applying neutral rectangle features to each facial expression: (a) the selected feature that distinguishes a neutral facial expression with the least error from other expressions in using the Viola-Jones features, (b) the selected feature that distinguishes a neutral facial expression with the least error from other expressions using the proposed rectangle features

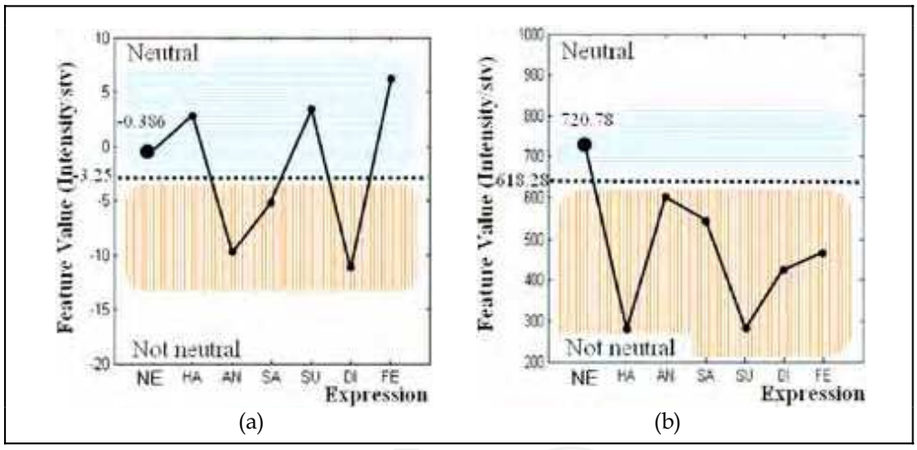

Figure 7. Comparison of feature values in applying a neutral rectangle feature to each facial expression: (a) using the Viola-Jones features, (b) using the proposed features

4. Facial Expression Generation

There are several projects that focus on the development of robotic faces. Robotic faces are currently classified in terms of their appearance; that is, whether they appear real, mechanical or mascot-like. In brief, this classification is based on the existence and flexibility of the robot's skin. The real type of robot has flexible skin, the mechanical type has no skin, and the mascot type has hard skin. Note that although there are many other valuable robotic faces in the world, we could not discuss all robots in this paper because space is limited.

In the real type of robot, there are two representative robotic faces: namely, Saya and Leonardo. Researchers at the Science University of Tokyo developed Saya, which is a

human-like robotic face. The robotic face, which typically resembles a Japanese woman, has hair, teeth, silicone skin, and a large number of control points. Each control point is mapped to a facial action unit (AU) of a human face. The facial AUs characterize how each facial muscle or combination of facial muscles adjusts the skin and facial features to produce human expressions and facial movements (Ekman et al., 2001) (Ekman & Friesen, 2003). With the aid of a camera mounted in the left eyeball, the robotic face can recognize and produce a predefined set of emotive facial expressions (Hara et al., 2001).

In collaboration with the Stan Winston studio, the researchers of Breazeal's laboratory at the Massachusetts Institute of Technology developed the quite realistic robot Leonardo. The studio's artistry and expertise of creating life-like animalistic characters was used to enhance socially intelligent robots. Capable of near-human facial expressions, Leonardo has 61 degrees of freedom (DOFs), 32 of which are in the face alone. It also has 61 motors and a small 16 channel motion control module in an extremely small volume. Moreover, it stands at about 2.5 feet tall, and is one of the most complex and expressive robots ever built (Breazeal, 2002).

With respect to the mechanical looking robot, we must consider the following well-developed robotic faces. Researchers at Takanishi's laboratory developed a robot called the Waseda Eye No.4 or WE-4, which can communicate naturally with humans by expressing human-like emotions. WE-4 has 59 DOFs, 26 of which are in the face. It also has many sensors which serve as sensory organs that can detect extrinsic stimuli such as visual, auditory, cutaneous and olfactory stimuli. WE-4 can also make facial expressions by using its eyebrows, lips, jaw and facial color. The eyebrows consist of flexible sponges, and each eyebrow has four DOFs. For the robot's lips, spindle-shaped springs are used. The lips change their shape by pulling from four directions, and the robot's jaw, which has one DOF, opens and closes the lips. In addition, red and blue electroluminescence sheets are applied to the cheeks, enabling the robot to express red and pale facial colors (Miwa et al., 2002) (Miwa et al., 2003).

Before developing Leonardo, Breazeal's research group at the Massachusetts Institute of Technology developed an expressive anthropomorphic robot called Kismet, which engages people in natural and expressive face-to-face interaction. Kismet perceives a variety of natural social cues from visual and auditory channels, and it delivers social signals to the human caregiver through gaze direction, facial expression, body posture, and vocal babbling. With 15 DOFs, the face of the robot displays a wide assortment of facial expressions which, among other communicative purposes, reflect its emotional state. Kismet's ears have 2 DOFs each; as a result, Kismet can perk its ears in an interested fashion or fold them back in a manner reminiscent of an angry animal. Kismet can also lower each eyebrow, furrow them in frustration, elevate them for surprise, or slant the inner corner of the brow upwards for sadness. Each eyelid can be opened and closed independently, enabling Kismet to wink or blink its eyes. Kismet also has four lip actuators, one at each corner of the mouth; the lips can therefore be curled upwards for a smile or downwards for a frown. Finally, Kismet's jaw has a single DOF (Breazeal, 2002).

The mascot-like robot is represented by a facial robot called Pearl, which was developed at Carnegie Mellon University. Focused on robotic technology for the elderly, the goal of this project is to develop robots that can provide a mobile and personal service for elderly people who suffer from chronic disorders. The robot provides a research platform of social interaction by using a facial robot. However, because this project is aimed at assisting

elderly people, the functions of the robot are focused more on mobility and auditory emotional expressions than on emotive facial expressions.

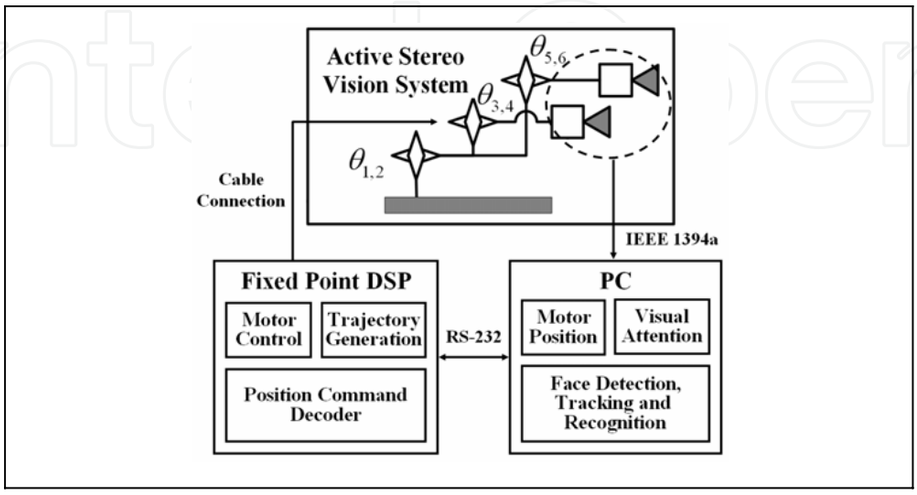

Figure 8. The whole system architecture. The image processing runs on a personal computer (PC) with a commercial microprocessor. In addition, the motion controller operates in a fixed point digital signal processor (DSP). An interface board with a floating point DSP decodes motor position commands and transfers camera images to the PC

Another mascot-like robot called ICat was developed by Philips. This robot is an experimentation platform for human-robot interaction research. ICat can generate many different facial expressions such as happiness, surprise, anger, and sad needed to make the human-robot interactions social. Unfortunately, there is no deep research of emotion models, relation between emotion and facial expressions, and emotional space.

4.1 System Description

The system architecture in this study is designed to meet the challenges of real-time visual-signal processing (nearly 30Hz) and a real-time position control of all actuators (1KHz) with minimal latencies. Ulkni is the name given to the proposed robot. Its vision system is built around a 3 GHz commercial PC. Ulkni's motivational and behavioral systems run on a TMS320F2812 processor and 12 internal position controllers of commercial RC servos. The cameras in the eyes are connected to the PC by an IEEE 1394a interface, and all position commands of the actuators are sent by the RS-232 protocol (see Fig. 8). Ulkni has 12 degrees of freedom (DOF) to control its gaze direction, two DOF for its neck, four DOF for its eyes, and six DOF for other expressive facial components, in this case the eyelids and lips (see Fig. 9). The positions of the proposed robot's eyes and neck are important for gazing toward a target of its attention, especially a human face. The control scheme for this robot is based on a distributed control method owing to RC servos. A commercial RC servo generally has an internal controller; therefore, the position of a RC servo is easily controlled by feeding a signal with a proper pulse width to indicate the desired position, and by then letting the internal controller operate until the current position of the RC servo reaches the desired position.

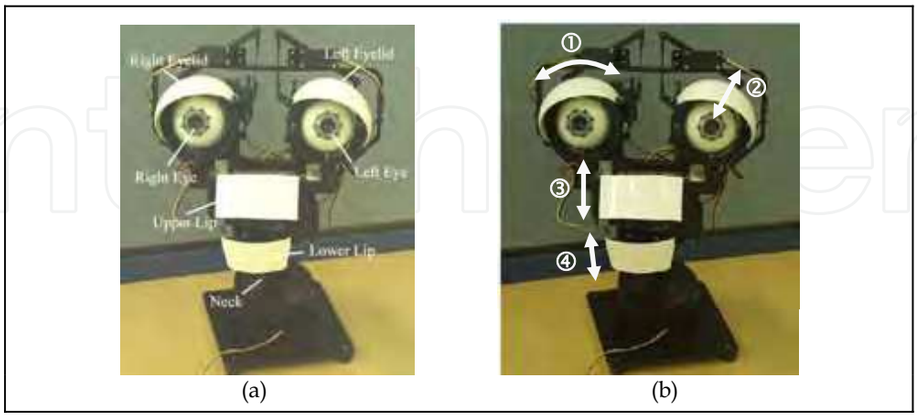

Figure 9. Ulkni's mechanisms. The system has 12 degrees of freedom (DOF). The eyes and the neck can pan and tilt independently. The eyelids also have two DOFs to roll and to blink. The lips can tilt independently. In Ulkni, rotational movements of the eyelids, ①, display the emotion instead of eyebrows. Ulkni's eyelids can droop and it can also squint and close its eyes, ②. Ulkni can smile thanks to the curvature of its lips, ③ and ④

Two objectives of the development of this robot in a control sense were to reduce the jerking motion and to determine the trajectories of the 12 actuators in real time. For this reason, the use of a high-speed, bell-shaped velocity profile of a position trajectory generator was incorporated in order to reduce the magnitude of any jerking motion and to control the 12 actuators in real time. Whenever the target position of an actuator changes drastically, the actuator frequently experiences a severe jerking motion. The jerking motion causes electric noise in the system's power source, worsening the system's controller. It also breaks down mechanical components. The proposed control method for reducing the jerking motion is essentially equal to a bell-shaped velocity profile. In developing the bell-shaped velocity profile, a cosine function was used, as a sinusoidal function is infinitely differentiable. As a result, the control algorithm ensures that the computation time necessary to control the 12 actuators in real time is achieved.

4.2 Control Scheme

Our control scheme is based on the distributed control method owing to RC servos. A commercial RC servo generally has an internal controller. Therefore, the position of a RC servo is easily controlled by feeding the signal that has the proper pulse width, which indicates a desired position, to the RC servo and then letting the internal controller operate until the current position of an RC servo reaches the desired position.

As mentioned above, if the target position of an actuator is changed drastically, severe jerking motion of the actuator will occur frequently. Jerking motions would cause electric noise in the power source of the system, worsen the controller of the system, and break down mechanical components. Therefore, our goal is to reduce or eliminate all jerking motion, if possible.

There have been some previous suggestions on how to solve the problems caused by jerking motion. Lloyd proposed the trajectory generating method, using blend functions (Lloyd & Hayward, 1991). Bazaz proposed a trajectory generator, based on a low-order spline method

(Bazaz & Tondu, 1999). Macfarlane proposed a trajectory generating method using an s-curve acceleration function (Macfarlane & Croft, 2001). Nevertheless, these previous methods spend a large amount of computation time on calculating an actuator's trajectory. Therefore, none of these methods would enable real-time control of our robot, Ulkni, which has 12 actuators.

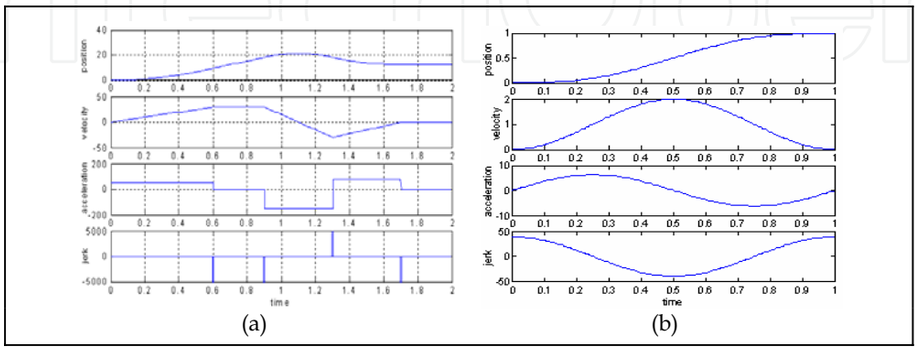

Figure 10. Comparison between the typical velocity control and the proposed bell-shaped velocity control: (a) trajectories of motor position, velocity, acceleration, and jerking motion with conventional velocity control, (b) trajectories of those with the proposed bell-shaped velocity control using a sinusoidal function

The two objectives of our research are to reduce jerking motion and to determine the trajectories of twelve actuators in real-time. Therefore, we propose a position trajectory generator using a high-speed, bell-shaped velocity profile, to reduce the magnitude of any jerking motion and to control twelve actuators in real-time. In this section, we will describe the method involved in achieving our objectives.

Fast Bell-shaped Velocity Profile

The bigger the magnitude of jerking motion is, the bigger the variation of acceleration is (Tanaka et al., 1999). Therefore, we can say that reducing the jerking motion is that the function of acceleration should be differentiable.

Presently, nearly all of the position control methods use a trapezoid velocity profile to generate position trajectories. Such methods are based on the assumption of uniform acceleration. Uniform acceleration causes the magnitude of jerking motion to be quite large. If the function of acceleration is not differentiable in any period of time an almost infinite magnitude of jerking motion will occur. Therefore, we should generate a velocity profile with a differentiable acceleration of an actuator (see Fig. 10).

Currently, researchers working with intelligent systems are trying to construct an adequate analysis of human motion. Human beings can grab and reach objects naturally and smoothly. Specifically, humans can track and grab an object smoothly even if the object is moving fast. Some researchers working on the analysis of human motion have begun to model certain kinds of human motions. In the course of such research, it has been discovered that the tips of a human's fingers move with a bell-shaped velocity profile when a human is trying to grab a moving object (Gutman et al., 1992). A bell-shaped velocity is generally differentiable. Therefore, the magnitude of jerking motion is not large and the position of an actuator changes smoothly.

We denote the time by the variable t, the position of an actuator at time t by the variable $p(t)$, the velocity of that at time t by the variable $v(t)$, the acceleration of that at time t by the variable $a(t)$, the goal position by the variable p_T, and the time taken to move the desired position by the variable T.
In (5), a previous model which has a bell-shaped velocity profile is shown.

$$\dot{a}(t) = -9\frac{a(t)}{T} - 36\frac{v(t)}{T^2} + 60\frac{(p_T - p(t))}{T^3} \tag{5}$$

The basic idea of our control method to reduce jerking motion is equal to a bell-shaped velocity profile. The proposed algorithm is used to achieve the computation time necessary to control twelve actuators in real-time. Therefore, we import a sinusoidal function because it is infinitely differentiable. We developed a bell-shaped velocity profile by using a cosine function. Assuming the normalized period of time is $0 \le t \le 1$, (6) shows the proposed bell-shaped velocity, the position, the acceleration, and the jerking motion of an actuator (see Fig. 10).
As seen in (6), the acceleration function, $a(t)$, is a differentiable, as well as the velocity function. Therefore, we can obtain a bounded jerk motion function. To implement this method, the position function, $p(t)$, is used in our system.

$$\begin{aligned} v(t) &= 1 - \cos 2\pi t \\ p(t) &= \int_0^1 v(t)\,dt = t - \frac{1}{2\pi}\sin 2\pi t \\ a(t) &= \frac{dv(t)}{dt} = 2\pi \sin 2\pi t \\ \dot{a}(t) &= \frac{da(t)}{dt} = 4\pi^2 \cos 2\pi t \end{aligned} \tag{6}$$

$$, \ where \ \ 0 \le t \le 1.$$

Finally, the developed system can be controlled in real-time even though target positions of 12 actuators are frequently changed. Some experimental results will be shown later.

4.3 Basic Function; Face Detection and Tracking

The face detection method is similar to that of Viola and Jones. Adaboost-based face detection has gained significant attention. It has a low computational cost and is robust to scale changes. Hence, it is considered as state-of-the-art in the face detection field.

AdaBoost-Based Face Detection

Viola et al. proposed a number of rectangular features for the detection of a human face in real-time (Viola & Jones, 2001) (Jones & Viola, 2003). These simple and efficient rectangular features are used here for the real-time initial face detection. Using a small number of important rectangle features selected and trained by AdaBoost learning algorithm, it was possible to detect the position, size and view of a face correctly. In this detection method, the value of rectangle features is calculated by the difference between the sum of intensities

within the black box and those within the white box. In order to reduce the calculation time of the feature values, integral images are used here. Finally, the AdaBoost learning algorithm selects a small set of weak classifiers from a large number of potential features. Each stage of the boosting process, which selects a new weak classifier, can be viewed as a feature selection process. The AdaBoost algorithm provides an effective learning algorithm on generalization performance.

The implemented initial face detection framework of our robot is designed to handle frontal views (-20~+20 [deg]).

Face Tracking

The face tracking scheme proposed here is a simple successive face detection within a reduced search window for real-time performance. The search for the new face location in the current frame starts at the detected location of the face in the previous frame. The size of the search window is four times bigger than that of the detected face.

4.4 Visual Attention

Gaze direction is a powerful social cue that people use to determine what interests others. By directing the robot's gaze to the visual target, the person interacting with the robot can accurately use the robot's gaze as an indicator of what the robot is attending to. This greatly facilitates the interpretation and readability of the robot's behavior, as the robot reacts specifically to the thing that it is looking at. In this paper, the focus is on the basic behavior of the robot - the eye-contact - for human-robot interaction. The head-eye control system uses the centroid of the face region of the user as the target of interest. The head-eye control process acts on the data from the attention process to center on the eyes on the face region within the visual field.

In an active stereo vision system, it is assumed for the purposes of this study that joint angles, $\boldsymbol{\theta} \in \mathbf{R}^{n\times 1}$, are divided into those for the right camera, $\boldsymbol{\theta}_r \in \mathbf{R}^{n_1\times 1}$, and those for the left camera, $\boldsymbol{\theta}_l \in \mathbf{R}^{n_2\times 1}$, where $n_1 \le n$ and $n_2 \le n$. For instance, if the right camera is mounted on an end-effector which is moving by joints 1, 2, 3, and 4, and the left camera is mounted on another end-effector which is moving by joints 1, 2, 5, and 6, the duplicated joints would be joints 1 and 2.

Robot Jacobian describes a velocity relation between joint angles and end-effectors. From this perspective, it can be said that Ulkni has two end-effectors equipped with two cameras, respectively. Therefore, the robot Jacobian relations are described as $\mathbf{v}_r = \mathbf{J}_r\dot{\boldsymbol{\theta}}_r$, $\mathbf{v}_l = \mathbf{J}_l\dot{\boldsymbol{\theta}}_l$ for the two end-effectors, where $\mathbf{v}_r$ and $\mathbf{v}_l$ are the right and the left end-effector velocities, respectively. Image Jacobian relations are $\dot{\mathbf{s}}_r = \mathbf{L}_r\mathbf{v}_r$ and $\dot{\mathbf{s}}_l = \mathbf{L}_l\mathbf{v}_l$ for the right and the left camera, respectively, where $\dot{\mathbf{s}}_r$ and $\dot{\mathbf{s}}_l$ are velocity vectors of image features, $\mathbf{L}_r$ and $\mathbf{L}_l$ are image Jacobian, and $\mathbf{v}_r$ and $\mathbf{v}_l$ may be the right and the left camera velocity if the cameras are located at the corresponding end-effectors. The image Jacobian is calculated for each feature point in the right and the left image, as in (7). In (7), Z is rough depth value of features and (x, y) is a feature position in a normalized image plane.

$$\mathbf{L}_{i=r,l} = \begin{pmatrix} -1/Z & 0 & x/Z & xy & -(1+x^2) & y \\ 0 & -1/Z & y/Z & 1+y^2 & -xy & -x \end{pmatrix} \tag{7}$$

In order to simplify control of the robotic system, it was assumed that the robot is a pan-tilt unit with redundant joints. For example, the panning motion of the right (left) camera is moved by joints 1 and 3(5), and tilt motion by joint 2 and 4(6). The interaction matrix is re-calculated as follows:

$$\dot{\mathbf{s}}_i = \tilde{\mathbf{L}}_i \dot{\boldsymbol{\theta}}_i, \tilde{\mathbf{L}}_i = \begin{pmatrix} xy & -(1+x^2) \\ 1+y^2 & -xy \end{pmatrix} \tag{8}$$

The visual attention task is identical to the task that is the canter of the detected face region to the image center. The visual attention task can be considered a regulation problem, $\dot{\mathbf{s}}_i = \mathbf{s}_i - \mathbf{0} = \mathbf{s}_i$. As a result, the joint angles are updated, as follows:

$$\begin{aligned} \dot{\boldsymbol{\theta}}_i &= \tilde{\mathbf{L}}_i^{+} \dot{\mathbf{s}}_i = \tilde{\mathbf{L}}_i^{+} \mathbf{s}_i \\ &= \frac{1}{x^2+y^2+1} \begin{pmatrix} -xy & 1+x^2 \\ \left(1+y^2\right) & xy \end{pmatrix} \begin{bmatrix} x \\ y \end{bmatrix} \\ &= \lambda(\mathbf{s}_i) \begin{pmatrix} y \\ -x \end{pmatrix} \end{aligned} \tag{9}$$

Two eyes are separately moved with a pan-tilt motion by the simple control law, as shown in (8). The neck of the robot is also moved by the control law in (9) with a different weight.

5. Experimental Results

5.1 Recognition Rate Comparison

The test database for the recognition rate comparison consists of a total of 407 frontal face images selected from the AR face database, PICS (The Psychological Image Collection at Stirling) database and Ekman's face database. Unlike the trained database, the test database was selected at random from the above facial image database. Consequently, the database has not only normal frontal face images, but also slightly rotated face images in plane and out of plane, faces with eye glasses, and faces with facial hair. Furthermore, whereas the training database consists of Japanese female face images, the test database is comprised of all races. As a result, the recognition rate is not sufficiently high because we do not consider image rotation and other races. However, it can be used to compare the results of the 7 rectangle feature types and those of the 42 rectangle feature types. Fig. 11 shows the recognition rate for each facial expression and the recognition comparison results of the 7 rectangle feature case and the 42 rectangle feature case using the test database. In Fig. 11, emotions are indicated in abbreviated form. For example, NE is neutral facial expression and HA is happy facial expression. As seen in Fig. 11, happy and surprised expressions show facial features having higher recognition rate than other facial expressions.

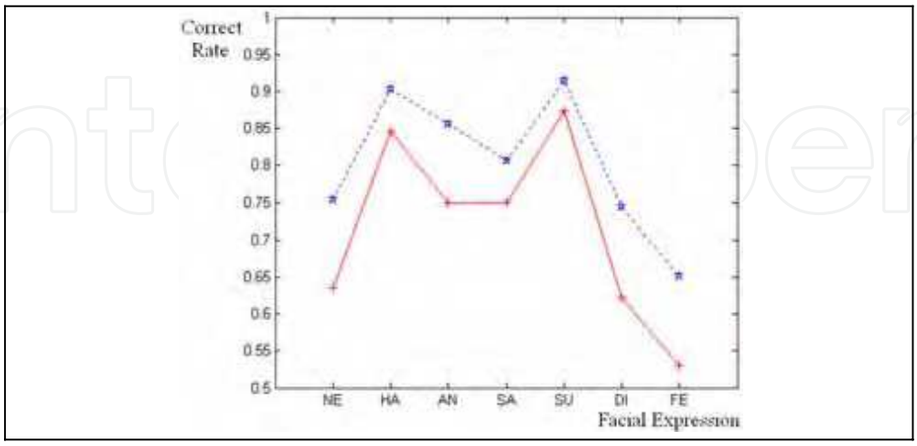

Figure 11. Comparison of the rate of facial expression recognition; '+' line shows the correct rate of each facial expression in case of 7 (Viola's) feature types, '*' line shows the correct rate of each facial expression in case of the proposed 42 feature types

In total, the 7 rectangle feature case has a lower recognition rate than the 42 rectangle feature case. For emotion, the difference ranges from 5% to 10% in the recognition rate. As indicated by the above results, it is more efficient to use 42 types of rectangle features than 7 rectangle features when training face images.

5.2 Processing Time Results

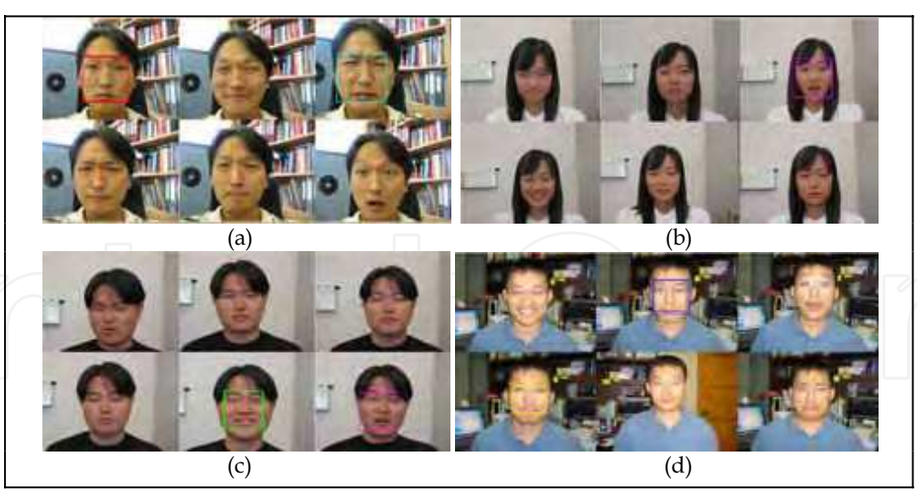

Figure 12. Facial expression recognition experiment from various facial expressions

Our system uses a Pentium IV, 2.8GHz CPU and obtains 320×240 input images from a camera. 250~300ms are required for a face to be detected for the case of an input image

where the face is directed forward. In the process of initial face detection, the system searches the entire input image area (320×240 pixels) and selects a candidate region and then performs pattern classification in the candidate region. As such, this takes longer than face tracking. Once the face is detected, the system searches the face in the tracking window. This reduces the processing time remarkably. Finally, when the face is detected, the system can deal with 20~25 image frames per second.

Figure 13. Facial expression recognition results. These photos are captured at frame 0, 30, 60, 90, 120, 150, 180 and 210 respectively (about 20 frames/sec)

5.2 Facial Expression Recognition Experiments

In Fig. 12, the test images are made by merging 6 facial expression images into one image.

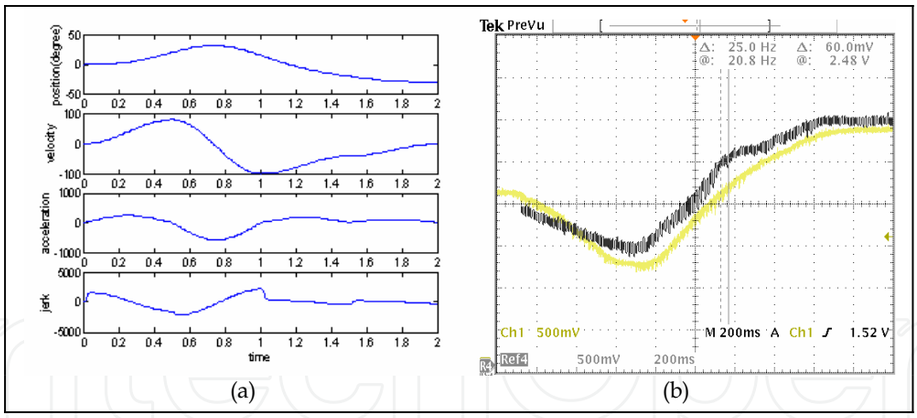

Figure 14. The initial position of an actuator is zero. Three goal positions are commanded at times 0, 1, and 1.5 seconds respectively: $p_T(0)=40$, $p_T(1)=10$, $p_T(1.5)=-30$. The velocity function can be obtained by merging the three bell-shaped velocity profiles, which are created at 0, 1, and 1.5 seconds, respectively: (a) simulation results and (b) experimental results

We then attempted to find specific facial expressions. Neutral and disgusted facial expressions are shown in Fig. 12(a), neutral and surprised facial expressions in Fig. 12(b),

happy and surprised facial expressions in Fig. 12(c) and angry and sad facial expressions in 12(d). It can be seen that the target facial expressions are detected. Fast processing time can be an essential factor for a facial expression recognition system since the facial expression may last only in a few seconds. Thus, we did the experiments for the sequential facial expression images. Fig. 13 shows the process of recognizing 7 facial expressions (neutral, happiness, anger, sadness, surprise, disgust, fear) in order.

5.3 Facial Expression Generation

First, we evaluated the proposed jerk-minimized control method to one joint actuator. The initial position of an actuator is zero, $p(0)=0$. Then, we commanded three goal positions: 40, 10, and -30, at 0 second, 1 second, and 1.5 seconds respectively. That is, $p_T(0)=40$, $p_T(1)=10$, $p_T(1.5)=-30$. Depicting this situation, Figure 14(a) shows the simulation results, which are calculated by Matlab, and Figure 14(b) shows the experimental results, with a comparison between the previous method, using a trapezoid velocity profile, and the proposed method, using a fast bell-shaped velocity profile. Figure 14(a) illustrates that there is less noise than in the previous method and the position trajectory of the motor is smoother than that of the previous method. In addition, an infinite magnitude of jerking motion is not found in Figure 14(b). That is, the magnitude of jerking motion is bounded within the limited area.

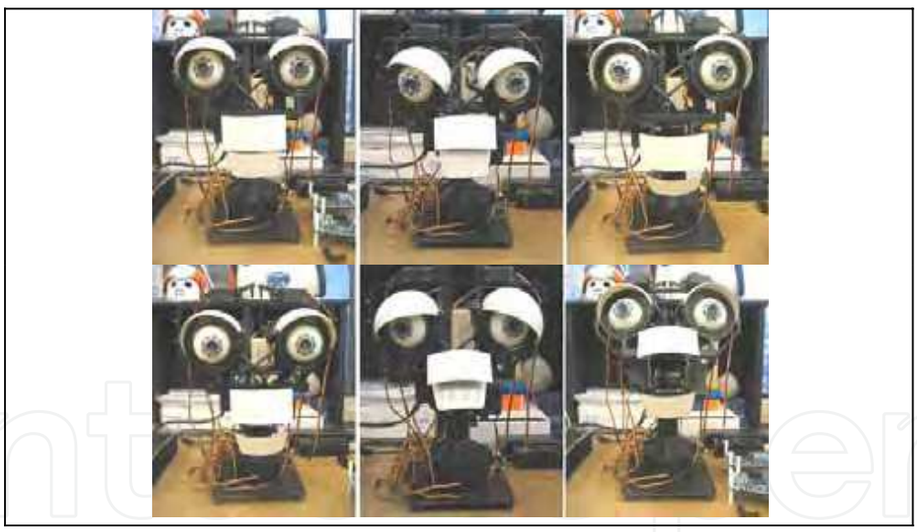

Figure 15. Ulkni's various facial expressions. There are 6 facial expressions which show his status; neutral, anger, happiness, fear, sadness, and surprise from the left-top to the right-bottom

Ulkni is composed of 12 RC servos, with four degrees of freedom (DOF) to control its gaze direction, two DOF for its neck, and six DOF for its eyelids and lips. Figure 15 shows the experimental results of the facial expression generation, such as normality, surprise,

drowsiness, anger, happiness, winsomeness. To express these kinds of facial expressions, we used the distributed control structure and the proposed fast bell-shaped velocity profiler. Our control scheme can simultaneously move the 12 actuators of our robot, Ulkni, in real-time and minimize the jerking motion of the actuators. The controller can update a desired change of position easily and smoothly, even if an actuator has not reached the previous goal position yet.

6. Conclusion

This Chapter has attempted to deal with the issues on establishing a facial expression imitation system for natural and intuitive interactions with humans. Several real-time cognition abilities are implemented to a robotic system such as face detection, face tracking, and facial expression recognition. Moreover, a robotic system with facial components is developed, which is able to imitate human's facial expressions.

A method of recognizing facial expressions is proposed through the use of an innovative rectangle feature. Using the AdaBoost algorithm, an expanded version of Viola and Jones' method has been suggested as a new approach. We deal with 7 facial expressions: neutral, happiness, anger, sadness, surprise, disgust, and fear. For each facial expression, we found five suitable rectangle features using the AdaBoost learning algorithm. These 35 rectangle features and 7 rectangle features were used to find new weak classifiers for facial expression recognition. A real-time performance rate can be achieved through constructing the strong classifier while extracting a few efficient weak classifiers by AdaBoost learning.

In addition, an active vision system for social interaction with humans is developed. We proposed a high-speed bell-shaped velocity profiler to reduce the magnitude of jerking motion and used this method to control 12 actuators in real-time. We proved our distributed control structure and the proposed fast bell-shaped velocity profiler to be practical. Several basic algorithms, face detection and tracking, are implemented on the developed system.

By directing the robot's gaze to the visual target, the person interacting with the robot can accurately use the robot's gaze as an indicator of what the robot is attending to. This greatly facilitates the interpretation and readability of the robot's behavior, as the robot reacts specifically to the thing that it is looking at. In order to implement visual attention, the basic functionality mentioned above, e.g. face detection, tracking and motor control, is needed.

Finally, we introduced an artificial facial expression imitation system using a robot head. There are a number of real-time issues for developing the robotic system. In this Chapter, one solution for developing it is addressed. Our final goal of this research is that humans can easily perceive motor actions semantically and intuitively, regardless of what the robot intends. However, our research lacks a sound understanding of natural and intuitive social interactions among humans. Our future research will focus on perceiving the mental model of human to apply it to the robotic system. It is expected that the suitable mental model for the robots will convey robot's emotion by facial expressions.

7. References

Bartlett, M. S. (1998). *Face Image Analysis by Unsupervised Learning and Redundancy Reduction*, PhD thesis, Universiy of California, San Diego.

Bazaz, S. & Tondu, B. (1999). Minimum Time On-line Joint Trajectory Generator Based on Low Order Spline Method for Industrial Manipulators, *Robotics and Autonomous Systems*, Vol. 29, pp. 257-268.

Breazeal, C. (2002). *Designing Sociable Robots*, MIT Press, Cambridge, MA, USA

Ekman, P.; Friesen, W. V. & Hager, J. C. (2002). *Facial Action Coding System*, Human Face, Salt Lake, Utah, USA

Ekman, P. & Friesen, W. V. (2003). *Unmasking the Face*, Malor Books, Cambridge, MA, USA.

Essa I. A. & Pentland A. P. (1997). Coding, Analysis, Interpretation, and Recognition of Facial Expressions, *IEEE Transaction on Pattern Analysis and Machine Intelligence*, Vol. 19, No. 7, pp. 757-763.

Fasel, B. & Luettin, J. (2003). Automatic Facial Expression Analysis: A Survey, *Pattern Recognition*, Vol. 36, No. 1, pp. 259-275.

Fellenz, W. A.; Taylor, J. G.; Tsapatsoulis, N. & Kollias, S. (1999). Comparing Template-Based, Feature-Based and Supervised Classification of Facial Expressions form Static Images, *Proceedings of Circuits, Systems, Communications and Computers*, pp. 5331-5336.

Freund, Y. & Schapire, R. E. (1995). A Decision-theoretic Generalization of On-line Learning and an Application to Boosting, *Computational Learning Theory: Eurocolt'95*, pp. 23-37.

Gutman, S. R.; Gottlieb, G. & Corcos, D. (1992). Exponential Model of a Reaching Movement Trajectory with Nonlinear Time, *Comments Theoretical Biology*, Vol. 2, No. 5, pp. 357-383.

Hara, F.; Akazawa, H. & Kobayashi, H. (2001). Realistic Facial Expressions by SMA Driven Face Robot, *Proceedings of IEEE Int. Workshop on Robot and Human Interactive Communication*, pp. 504-511.

Huang, C. L. & Huang, Y. M. (1997). Facial Expression Recognition using Model-Based Feature Extraction and Action Parameters Calssification, *Journal of Visual Communication and Image Representation*, Vol. 8, No. 3, pp. 278-290.

Jones, M. & Viola, P. (2003). Fast Multi-View Face Detection. *Technical Report of Mitsubishi Electric Research Laboratory*: TR-2003-96, USA.

Kim, D. H.; Lee, H. S. & Chung, M. J. (2005). Biologically Inspired Models and Hardware for Emotive Facial Expressions, *Proceedings of IEEE Int. Workshop Robot and Human Interactive Communication,* pp. 680-685, Tennessee, USA

Lanitis, A.; Taylor, C. J. & Cootes, T. F. (1997). Automatic Interpretation and Coding of Face Images using Flexible Models, *IEEE Transaction on Pattern Analysis and Machine Intelligence*, Vol 19, No, 7, pp. 743-756.

Lien, J. J.; Kanade, T.; Cohn, J. F. & Li, C-C. (1998). Automated Facial Expression Recognition Based FACS Action Units, *Proceedings of IEEE International Conference on Automatic Face and Gesture Recognition*, pp. 390-395.

Lisetti, C. L. & Rumelhart, D. E. (1998). Facial Expression Recognition using a Neural Network, *Proceedings of the International Flairs Conference*. AAAI Press.

Littlewort, G. C.; Bartlett, M. S.; Chenu, J.; Fasel, I.; Kanda, T.; Ishiguro, H. & Movellan, J. R. (2004). Towards Social Robots: Automatic Evaluation of Human-Robot Interaction by Face Detection and Expression Classification, In: *Advances in Neural Information Processing Systems*, S. Thrun, L. Saul and B. Schoelkopf, (Eds.), Vol 16, pp. 1563-1570, MIT Press.

Lloyd, J. & Hayward, V. (1991). Real-Time Trajectory Generation Using Blend Functions, *Proceedings of IEEE Int. Conf. Robotics and Automation*, pp. 784-789.

Macfarlane, S. & Croft, E. (2001). Design of Jerk Bounded Trajectories for On-line Industrial Robot Applications, *Proceedings of IEEE Int. Conf. Robotics and Automation*, pp. 979-984.

Miwa, H.; Okuchi, T.; Takanobu, H. & Takanishi, A. (2002). Development of a New Human-like Head Robot WE-4, *Proceedings of IEEE/RSJ Int. Conf. on Intelligent Robots and Systems*, pp. 2443-2448.

Miwa, H.; Okuchi, T.; Itoh, K.; Takanobu, H. & Takanishi, A. (2003). A New Mental Model for Humanoid Robots for Human Friendly Communication, *Proceedings of IEEE Int. Conf. on Robotics and Automation*, pp. 3588-3593.

Mcneill, D. (1998). *The Face*, Little, Brown & Company, Boston, USA

Padgett, C. & Cottrell, G. W. (1997). Representing Face Image for Emotion Classification, In: *Advances in Neural Information Proceessing Systems*, M. Mozer, M. Jordan, and T. Petsche, (Eds.), Vol. 9, pp. 894-900, MIT Press.

Pantic, M. & Rothkrantz, L. J. M. (2000). Automatic Analysis of Facial Expression: the State of Art, *IEEE Transaction on Pattern Analysis and Machine Intelligence*, Vol. 22, No. 12, pp. 1424-1445.

Tanaka, Y.; Tsuji, T. & Kaneko, M. (1999). Bio-mimetic Trajectory Generation of Robotics using Time Base Generator, *Proceedings of IEEE Int. Conf. Intelligent Robots and Systems*, pp. 1301-1315.

Viola, P. & Jones, M. (2001). Rapid Object Detection using a Boosted Cascade of Simple Features, *Proceedings of IEEE International Conference on Computer Vision and Pattern Recognition*, pp. 511-518.

Wang, Y.; Ai, H.; Wu, B. & Huang, C. (2004). Real Time Facial Expression Recognition with Adaboost, *Proceedings of IEEE International Conference on Pattern Recognition*, vol. 3, pp. 926-929.

Zhang, Z.; Lyons, M.; Schuster, M. & Akamatsu, S. (1998). Comparision between Geometry-Based and Gabor-Wavelets-Based Facial Expression Recognition using Multi-Layer Perceptron, *Proceedings of IEEE International Conference on Automatic Face and Gesture Recognition*, pp. 454-459.

Human Robot Interaction

Edited by Nilanjan Sarkar

ISBN 978-3-902613-13-4

Hard cover, 522 pages

Publisher I-Tech Education and Publishing

Published online 01, September, 2007

Published in print edition September, 2007

Human-robot interaction research is diverse and covers a wide range of topics. All aspects of human factors and robotics are within the purview of HRI research so far as they provide insight into how to improve our understanding in developing effective tools, protocols, and systems to enhance HRI. For example, a significant research effort is being devoted to designing human-robot interface that makes it easier for the people to interact with robots. HRI is an extremely active research field where new and important work is being published at a fast pace. It is neither possible nor is it our intention to cover every important work in this important research field in one volume. However, we believe that HRI as a research field has matured enough to merit a compilation of the outstanding work in the field in the form of a book. This book, which presents outstanding work from the leading HRI researchers covering a wide spectrum of topics, is an effort to capture and present some of the important contributions in HRI in one volume. We hope that this book will benefit both experts and novice and provide a thorough understanding of the exciting field of HRI.

InTech Europe

University Campus STeP Ri
Slavka Krautzeka 83/A
51000 Rijeka, Croatia
Phone: +385 (51) 770 447
Fax: +385 (51) 686 166
www.intechopen.com

InTech China

Unit 405, Office Block, Hotel Equatorial Shanghai
No.65, Yan An Road (West), Shanghai, 200040, China
中国上海市延安西路65号上海国际贵都大饭店办公楼405单元
Phone: +86-21-62489820
Fax: +86-21-62489821

IntechOpen